Physica C 469 (2009) 614–627

Contents lists available at ScienceDirect

Physica C

journal homepage: www.elsevier.com/locate/physc

Pairing symmetry and pairing state in ferropnictides: Theoretical overview

I.I. Mazin [a,*], J. Schmalian [b]

[a] Code 6391, Naval Research Laboratory, Washington, DC 20375, United States
[b] Iowa State University and Ames Laboratory, Ames, IA 50011, United States

ARTICLE INFO

Article history:
Available online 19 March 2009

PACS:
74. 74.20.–z
74.20.Mn
74.20.Rp

Keywords:
Unconventional superconductivity
Pnictides
Superconductivity and magnetism

ABSTRACT

We review the main ingredients for an unconventional pairing state in the ferropnictides, with particular emphasis on interband pairing due to magnetic fluctuations. Summarizing the key experimental prerequisites for such pairing, the electronic structure and nature of magnetic excitations, we discuss the properties of the $s^{\pm}$ state that emerges as a likely candidate pairing state for these materials and survey experimental evidence in favor of and against this novel state of matter.

Published by Elsevier B.V.

One fist of iron, the other of steel.
If the right one don't get you, then the left one will / *Merle Travis, 16 tons*

1. Introduction

The discovery of cuprate superconductors has changed our mentality in many ways. In particular, the question that would have sounded moot to most before 1988, *what is the symmetry of the superconducting state*, is now the first question to be asked when a new superconductor has been discovered. The pool of potential candidates, before considered at best a mental Tetris for theorists, had acquired a practical meaning. It has been demonstrated that superconductivity in cuprates is *d*-wave, while in MgB_2 it is multi-gap *s*-wave with a large gap disparity. There is considerable evidence that Sr_2RuO_4 is a *p*-wave material. Other complex order parameters are routinely discussed for heavy fermion systems or organic charge transfer salts. It is likely that the newly discovered ferropnictides represent another superconducting state, not encountered in experiment before.

Besides the general appreciation that pairing states may be rather nontrivial, it has also been recognized that unconventional pairing is likely due, at least to some extent, to electronic (Coulomb or magnetic) mechanisms and, conversely, electronic mechanisms are much more likely to produce unconventional pairing symmetries than the standard uniform-gap *s*-wave. It has been appreciated that the actual symmetry is very sensitive to the momentum dependence of the pairing interaction, as well as to the underlying electronic structure (mostly, fermiology).

Therefore we have structured this overview so that it starts with a layout of prerequisites for a meaningful discussion of the pairing symmetry. First of all, we shall describe the gross features of the fermiology according to density-functional (DFT) calculations, as well as briefly assess verification of such calculations *via* ARPES and quantum oscillations experiments. Detailed discussion of these can be found elsewhere in this volume. We will also point out where one may expect caveats in using the DFT band structure: it is in our view misleading to assume that these compounds are uncorrelated. While not necessarily of the same nature as in cuprates, considerable electron–electron interaction effects cannot be excluded and are even expected.

We will then proceed to discuss the role of magnetic fluctuations as well as other excitations due to electron–electron interactions. We discuss the special role the antiferromagnetic (AFM) ordering vector plays for the pairing symmetry and address the on-site Coulomb (Hubbard correlations), to the extent of their possible effect on the pairing symmetry, and possible overscreening (Ginzburg–Little) interactions. We also discuss puzzling issues that are related to the magneto-elastic interaction in these systems. As for a discussion of the electron–phonon interaction we refer to the article by Boeri et al. in this volume. The final part of this review consists of a summary of theoretical aspects of the pairing state, along with a discussion of its experimental manifestations.

* Corresponding author.
E-mail address: maxin@nrl.navy.mil (I.I. Mazin).

0921-4534/$ - see front matter Published by Elsevier B.V.
doi:10.1016/j.physc.2009.03.019

2. Prerequisites for addressing the Cooper pairing

2.1. Electronic structure and fermiology

2.1.1. Density-functional calculations

The two main families of the Fe-based superconductors are 1111 systems ROFeAs with rare earth ions R [1,2] and the 122 systems AFe_2As_2 with alkaline earth element A [3]. Both families have been studied in much detail by first principles DFT calculations. Here and below, unless specifically indicated, we use a 2D unit cell with two Fe per cell, and the corresponding reciprocal lattice cell; the x and y directions are along the next-nearest-neighbor Fe–Fe bond. It appears that all materials share the same common motif: two or more hole-like Fermi surfaces near the Γ point [$\mathbf{k} = (0,0)$], and two electron-like surfaces near the M point [$\mathbf{k} = (\pi,\pi)$] (Figs. 1–5). This is true, however, in strictly nonmagnetic calculations only, when the magnetic moment on each Fe is restricted to zero. As discussed below, this is not necessarily a correct picture.

If, however, we neglect this potential caveat, and concentrate on the two best studied systems, 1111 and 122, the following relevant characteristics can be pointed out: First, the density of states (DOS) for holes and electrons is comparable for undoped materials; with doping, respectively one or the other becomes dominant. For instance, for $Ba_{0.6}K_{0.4}Fe_2As_2$ the calculated DOS (in the experimental structure) for the three hole bands varies between 1.1 st/eV/f.u. and 1.3 st/eV/f.u., the inner cylinder having, naturally, the smallest DOS and the outer the largest. For the electron bands the total DOS is 1.2 st/eV/f.u., that is, two to three times smaller than the total for the hole bands [4]. We shall see later that this is important. Another interesting effect is that in the 122 family doping in either direction strongly reduces the dimensionality compared to undoped compounds (in the 1111 family this effect exists, but is much less pronounced), see Fig. 4. This suggests that the reason that doping destroys the long-range magnetic order (it is believed by many that such a destruction is prerequisite for superconductivity in ferropnictides) is not primarily due to the change in the 2D electronic structure, as it was initially anticipated [5], but rather due to the destruction of magnetic coupling between the layers. Indeed the most striking difference between the undoped 1111 and undoped 122 electronic structure is quasi two-dimensionality of the former and a more 3D character of the latter (the difference is clear already in the paramagnetic calculations, but is particularly drastic in the antiferromagnetic state), while at the same time the observed magnetism in the 122 family is at least three times stronger than in LaFeAsO (in the mean-field DFT calculation the difference is quite small).

The fact that the nesting is very imperfect is crucial from the point of view of an SDW instability, making the material stable against infinitesimally small magnetic perturbation. For superconductivity, however, it is less important, as discussed later in the paper.

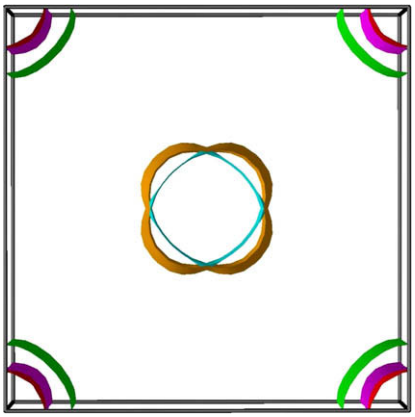

Fig. 1. The Fermi surface of the nonmagnetic LaAsFeO for 10% e-doping [4]. The main difference between the calculations using the experimental atomic positions, as here, and the calculated ones, as in Ref. [5], is presence of the third hole sheet (x^2-y^2 band).

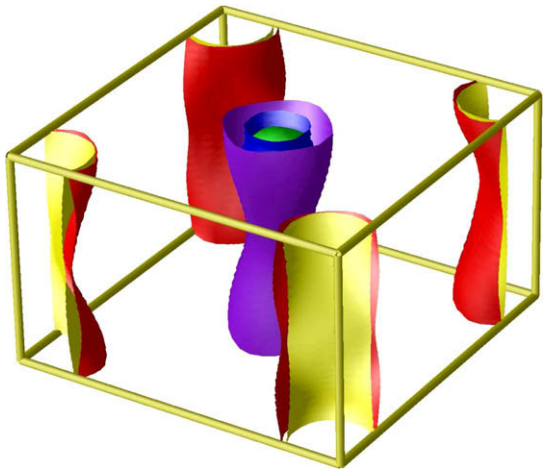

Fig. 2. The Fermi surface of the nonmagnetic $BaFe_2As_2$ for 10% e-doping (Co doping, virtual crystal approximation) [4].

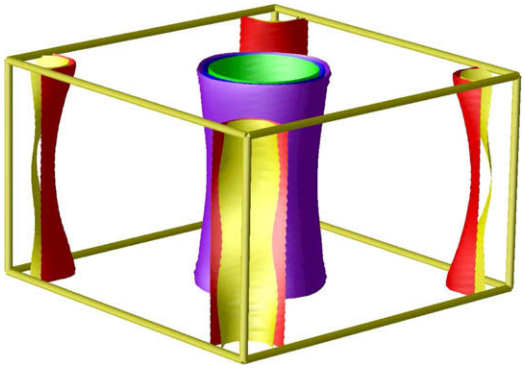

Fig. 3. The Fermi surface of the nonmagnetic $BaFe_2As_2$ for 10% h-doping (20% Cs doping, virtual crystal approximation [4])

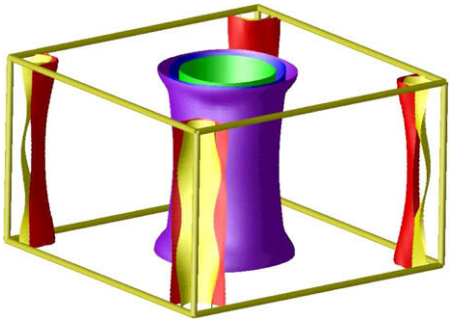

Fig. 4. The Fermi surface of $BaFe_2As_2$ for 20% h-doping (corresponding to $Ba_{1.6}K_{0.4}Fe_2As_2$, calculated as 40% Cs doping in the virtual crystal approximation) [4]. Note that, had we use the calculated As positions instead of the experimental ones, the FS would have been much more 3D.

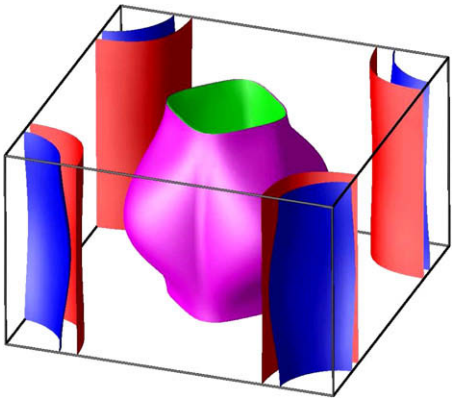

Fig. 5. The Fermi surface of undoped nonmagnetic FeTe. [4].

2.1.2. Experimental evidence

Experimental evidence regarding the band structure and fermiology of these materials comes, basically, from two sources: angular resolved photoemission spectroscopy (ARPES) and quantum oscillations measurements. The former has an additional advantage of being capable of probing the electronic structure in the superconducting state, assessing the amplitude and angular variation of the superconducting gap. A potential disadvantage is that it is a surface probe, and pnictides, especially the 122 family, are much more three-dimensional than cuprates. This means that, first, the in-plane bands as measured by ARPES, strongly depend on the normal momentum, $k_\perp$, and, second, there is a bigger danger of surface effects in the electronic structure than in the cuprates. There are indications that the at least in 1111 compounds the surface is charged, that is to say, the doping level in the bulk is different from that on the surface. Additionally, LDA calculations suggest that in the magnetic prototypes, the band structure depends substantially on interlayer magnetic ordering, again, not surprisingly, mostly in the 122 compounds, as Fig. 6 illustrates. Of course, there is no guarantee that the last two layers order in the same way as the bulk (or even with the same moment).

These caveats notwithstanding, ARPES has already provided invaluable information. ARPES measurements have been performed for both 1111 [6,7] and 122 materials [8–11]. These measurements demonstrated the existence of a well-defined Fermi surface that consists of hole and electron pockets, in qualitative agreement with the predictions of electronic structure calculations. Thus, one can say that the topology of the Fermi surface, including the location and the relative size of the individual Fermi surface sheets agrees with the LDA expectation — which is most important for the pairing models. Similarly, it is rather clear that the ARPES bandwidth is reduced from the LDA one by a factor of 2–2.5, similar to materials with strong itinerant magnetic fluctuations (*cf.*, for instance, Sr_2RuO_4 near a magnetic quantum critical point [12]). These findings are also consistent with the deduced normal state linear specific heat coefficient in 1111 materials (*e.g.,* 4–6 mJ/mol K^2 in Ref. [13]) corresponding to a factor 1–2 compared to the bare LDA value [14]. However, in the 122 compound a specific heat coefficient 63 mJ/mol K^2 was reported [13], to be compared with roughly 11.5 mJ/mol K^2 from the LDA calculations [4]. While a renormalization of 5.5 is not consistent with either ARPES or quantum oscillations, consistency among different experimental publications for the 122 systems is lacking as well [15,13].

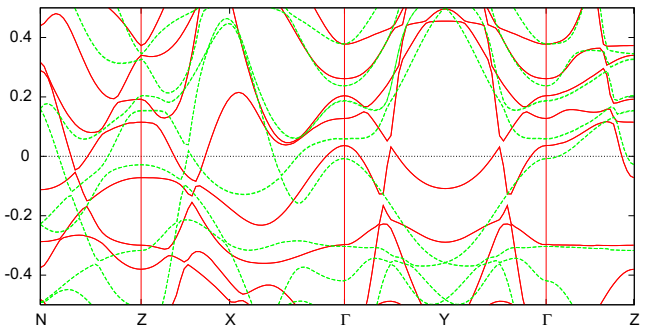

Fig. 6. Band structure of the orthorhombic antiferromagnetic $BaFe_2As_2$ calculated for two different interlayer ordering pattern: the experimental antiferromagnetic one (space group #66, broken green) and the hypothetical ferromagnetic (still antiferromagnetic in plane, space group #67, solid red). In both cases the magnetic moment on Fe was artifically suppressed to $1\mu_B$ by applying a fictitious negative Hubbard U [4]. The point N is above the point Y.

Another experimental probe of the electronic structure is based on quantum oscillations that measure extremal cross-section areas of the FS (ideally, for different directions of the applied field) and the effective masses. Such measurements are very sensitive to the sample quality, therefore so far only a handful of results are available. However, data on the P-based 1111 compound agree reasonably well with band structure calculations [16], and indicate the same mass renormalization as ARPES [17].

Importantly, quantum oscillations measurements on AFM 122 compounds [18,19] indicate that even the undoped pnictides are well-defined Fermi liquids, even though a significant portion of the Fermi surface disappears due to the opening of a magnetic gap. The frequencies of the magneto-oscillations then suggest that the ordered magnetic state has small Fermi surface pockets consistent with the formation of a spin-density wave. Thus, the electronic structure of the pnictides is consistent with a metallic state with well-defined Fermi surfaces.

Besides determining the overall shape of the Fermi surface sheets, ARPES is able to yield crucial information about the momentum dependence of the superconducting gap. Several groups performed high quality ARPES measurements to this effect [7–10]. In some cases significant differences in the size of the gap amplitude for different Fermi surface sheets have been observed. However, there seems to be a consensus between all ARPES groups that the gap amplitude on an individual Fermi surface sheet depends weakly on the direction. While this seems to favor a pairing state without nodes, one has to keep in mind that all measurements so far have been done for fixed values of the momentum $k_\perp$, perpendicular to the planes. While it might be premature to place too much emphasis on the relative magnitude of the gaps observed in different bands in ARPES experiments, it is worth noting that most experimentalists agree that in the hole-doped 122 material the inner hole barrel and the electron barrel have comparable (and large) superconducting gaps, while the outer hole barrel has about twice smaller gap. On the other hand, there are first data [20] indicating that in the electron-doped $BaFe_{1.85}Co_{0.15}As_2$ the hole and the electron bands have about the same gap despite the hole pockets shrinking, and electron pocket extending. Even more interesting, the most natural interpretation of the measured fermiology is that the hole FS in $BaFe_{1.85}Co_{0.15}As_2$ actually corresponds to the outer (xz/yz) barrel in $Ba_{0.6}K_{0.4}Fe_2As_2$ that has a small gap in that compound.

2.1.3. Role of spin fluctuations in electronic structure

As is clear from the above discussion, strong spin fluctuations have a substantial effect upon the band structure. First of all, they dress one-electron excitations providing mass renormalization, offering an explanation for the factor 2–2.5. This is in fact a relatively modest renormalization: it is believed that, for instance, in He^3 or in Sr_2RuO_4 itinerant spin fluctuations provide renormalization of a factor of 4 or larger. However, it is likely that the effect

goes beyond simple mass renormalization. As will be discussed in detail below, there is overwhelming evidence of large local moments on Fe, mostly from the fact that the Fe–As bond length corresponds to a fully magnetic (large) Fe ion. There is also evidence that the in-plane moments are rather well correlated in the planes, and the apparent loss of the long-range ordering above T_N is mainly due to a loss of 3D coherency between the planes [21]. It is only natural to expect a similar situation to be true when magnetism is suppressed by doping.

If that is the case, the electronic structure in the paramagnetic parts of the phase diagram, at least in the vicinity of the transition, should not be viewed as dressed nonmagnetic band, but rather as an average between the bands corresponding to various magnetic 3D stackings (*cf.* Fig. 6). Fig. 6, corresponding to the $T = 0$ magnetic moment of $1\mu_B$, is probably exaggerating this effect, but it is still likely that in a considerable range of temperatures and doping near the observed magnetic phase boundary a nonmagnetic band structure is not a good starting point, and a theory based on magnetic precursors is needed. More experiments, particularly using diffuse scattering, and more theoretical work are needed to clarify the issue. A discussion to this effect may be found in Ref. [22]. See also Section 2.3 below.

2.2. Magnetic excitations

2.2.1. Experimental evidence

Compared to cuprates and other similar compounds, two peculiarities strike the eye. First, the parent compounds of the pnictide superconductors assume an antiferromagnetic structure, where neighboring Fe moments are parallel along one direction within the FeAs plane and antiparallel along the other. Neutron scattering data yield ordered moments per Fe of $0.35\mu_B$ for LaFeAsO [23], $0.25\mu_B$ for NdFeAsO [24], $0.8\mu_B$ for CeFeAsO [25], and $0.9\mu_B$ for $BaFe_2As_2$ [26]. Intriguingly, in NdFeAsO the ordered moment at very low temperatures increases by a factor of 3–4 at the temperature corresponding to the ordering of Nd-spins [27]. Note that the correct magnetic structure has been theoretically predicted by DFT calculations [5,28], which, moreover, consistently overestimated the tendency to magnetism (as opposed to the cuprates). Second, the magnetically ordered state remains metallic. As opposed to cuprates or other transition metal oxides, the undoped systems exhibit a small but well established Drude conductivity [29], display magneto-oscillations [18] and have Fermi surface sheets of a partially gapped metallic antiferromagnetic state [30]. Above the magnetic ordering temperature a sizable Drude weight, not untypical for an almost semimetal, has been observed. Further, the ordered Fe magnetic moment in the 1111 systems depends sensitively on the rare earth ion, very different from $YBa_2Cu_3O_6$ where yttrium can be substituted by various rare earth elements with hardly any effect on the Cu moment. Note that the rare earth sites project onto the centers of the Fe plaquettes and thus do not exchange-couple with the latter by symmetry. Finally, the magnetic susceptibility of $BaFe_2As_2$ single crystals [31] above the magnetic transition shows no sign for an uncoupled local moment behavior.

2.2.2. Itinerant versus local magnetism

The vicinity of superconductivity to a magnetically ordered state is the key motivation to consider pairing mechanisms in the doped systems that are linked to magnetic degrees of freedom. Similar to cuprate superconductors, proposals for magnetic pairing range from quantum spin fluctuations of localized magnetic moments to fluctuations of paramagnons as expected in itinerant electron systems. To judge whether the magnetism of the parent compounds is localized or itinerant (or located in the crossover regime between these two extremes) is therefore crucial for the development of the correct description of magnetic excitations and possibly the pairing interactions in the doped systems.

In our view the case at hand is different from such extreme cases as undoped cuprates on one end and weak itinerant magnets like $ZrZn_2$ on the other. While being metals with partially gapped Fermi surface, there is evidence that Fe ions are in a strongly magnetic state with strong Hund rule coupling for Fe. This results in a large magnetic moment—but only for some particular ordering patterns (for comparison, in FeO and similar materials LDA produces large magnetic moment regardless of the imposed long-range order). While it is obvious that ferropnictides are not Mott insulators with localized spins, interacting solely with near neighbors, a noninteracting electron system may be not a perfect starting approximation either. To make progress we have to decide what is the lesser of two evils and use it, even realizing the problems with the selected approach. Given the above-mentioned experimental facts, our preference is that these systems are still on the itinerant side.

A feature that has attracted much interest is the quasi-nesting between the electron and the hole pockets. The word "quasi" is instrumental here: even the arguably most nested undoped LaFeAsO is very far from the ideal nesting and even worse in the (more magnetic) $BaFe_2As_2$. Indeed, it has been observed that in the LDA calculations the nonmagnetic structure in either compound is stable with respect to an infinitesimally small AFM perturbations, but strongly unstable with respect to finite amplitude perturbations. This can be understood from the point of view of the Stoner theory, applied to a finite wave vector $\mathbf{Q}$: the renormalized static spin susceptibility (in the DFT the RPA approximation is formally exact) can be written as

$$\chi_{LDA}(\mathbf{Q}) = \frac{\chi_0(\mathbf{Q})}{1 - I\chi_0(\mathbf{Q})}, \tag{1}$$

where I is the Stoner factor of iron, measuring the intra-atomic Hund interaction (in the DFT, it is defined by the second variation of the exchange-correlation functional with respect to the spin density). While the denominator in Eq. (1) provides a strong enhancement of χ, albeit not exactly at $\mathbf{Q} = (\pi, \pi)$, but at a range of the wave vectors near $\mathbf{Q}$, it does not by itself generate an instability. One can say that an infinitesimally weak magnetization can only open a gap over a very small fraction of the Fermi surface. However, a large-amplitude spin-density wave opens a gap of the order of the exchange splitting, IM, where M is the magnetic moment on iron, and, obviously, affects most of the conducting electrons. In other words, the magnetism itself is generated by the strong Hund rule coupling on Fe (just as in the metal iron), but the topology of the Fermi surface helps select the right ordering pattern. Formation of the magnetic moments is local; arranging them into a particular pattern is itinerant.

There are several corollaries of this fact that are important for pairing and superconductivity. First, despite the fact that the overall physics of these materials is more on the itinerant side than on the localized side (see a discussion to this effect later in the paper), it is more appropriate to consider magnetic moments on Fe as local rather than itinerant (as for instance in the classical spin-Peierls theory). Note that the same is true for the metal iron as well. Second, the *interaction* among these moments is *not* local, as for instance in superexchange systems (it appears impossible to map the energetics of the DFT calculations onto a two nearest neighbor Heisenberg model [32]). The AFM vector is not determined by local interactions in real space (as for instance in the $J_1 + J_2$ models, see below), but by the underlying electronic structure in reciprocal space. Third, since the energy gain due to formation of the SDW mainly occurs at finite (and large, IM is on the order of eV) energies, looking solely at the FS may be misleading. Indeed, FeTe is one

compound where the Fe moments apparently do not order into a $\mathbf{Q}=(\pi,\pi)$ SDW, but in a more complex structure corresponding to a different ordering vector [33], despite the fact that the FS shows about the same degree of nesting (Fig. 5) as LaFeAsO and a noticeably better nesting than $BaFe_2As_2$. DFT calculations correctly identify the ground state in all these cases, and the origin can be traced down again to the opening of a partial gap: in both 1111 and 122 compounds the $\mathbf{Q}=(\pi,\pi)$ is about the only pattern that opens such a gap around the Fermi level, while in FeTe comparable pseudogaps open in both magnetic structures (and the calculated energies are very close, the actual experimental structure being slightly lower [34]).

2.2.3. Perturbative itinerant approach

Even if one accepts the point of view that the magnetism in the Fe-pnictides is predominantly itinerant, the development of an adequate theory for the magnetic fluctuation spectrum is still highly nontrivial. As pointed out above, there are strong arguments that the driving force for magnetism is not Fermi surface nesting but rather a significant local Hund's and exchange coupling. This can be quantitatively described in terms of a multiband Hubbard type interaction of the Fe-3*d* states

$$H_{int} = U\sum_{i,a} n_{ia\uparrow}n_{ia\downarrow} + U'\sum_{i,a>b} n_{ia}n_{ib} - J_H\sum_{i,a>b}\left(2\mathbf{s}_{ia}\cdot\mathbf{s}_{ib}+\frac{1}{2}n_{ia}n_{ib}\right)+J\sum_{i,a>b,\sigma} d^\dagger_{ia\sigma}d^\dagger_{ia\bar{\sigma}}d_{ib\bar{\sigma}}d_{ib\sigma}, \qquad (2)$$

with intra- and inter-orbital Coulomb interaction U and U', Hund's coupling J_H and exchange coupling J, respectively. Here a, b refer to the orbitals in a Wannier type orbital at site i. X-ray absorption spectroscopy measurements support large values for the Hund's couplings that lead to a preferred high spin configuration, [35] leading to larger values of J_H. The importance of the Hund coupling for the normal state behavior of the pnictides was recently stressed in Ref. [36].

Weak-coupling expansions in these interaction parameters may not capture quantitative aspects of the magnetism in the pnictides. Nevertheless, it is instructive to summarize the main finding of the result of weak-coupling expansions, in particular as they demonstrate the very interesting and nontrivial aspects that results from interband interactions with almost nested hole and electron Fermi-surfaces [37–39]. For an ideal semimetal (two identical hole and electron bands with the Fermi energies E_h and E_e) all susceptibilities at the nesting vector $\mathbf{Q}$ diverge as $\log|E_h/E_e-1|$. Depending on the details of electron–electron interaction this signals an instability, at $E_h=E_e$, to a spin-density wave state or to a superconducting state for infinitesimal interaction. The corresponding interference between particle-hole and particle–particle scattering events can be analyzed by using a renormalization group approach. For $J_H=J=0$, the authors of Ref. [38] find that at low energies the interactions are dominated by Cooper pair-hopping between the two bands, favoring an $s^{\pm}$-superconducting state that is fully gapped on each Fermi surface sheet, but with opposite sign on the two sheets. It is worth pointing out that this pairing mechanism is due to very generic interband scattering, not necessarily due to *spin fluctuations*, as all particle-hole and particle–particle scattering events enter in essentially the same matter (a detailed discussion of this approach can be found in A. Chubukov's contribution to this volume). An $s^{\pm}$-state was also obtained using a functional renormalization group approach [37], where the authors argue that the pairing mechanism is due to collective spin fluctuations that generate a pairing interaction at low energies. The appeal of these calculations is clearly that controlled and thus robust conclusions can be drawn. On the other hand, as discussed below, the Fermi surface nesting is less crucial as is implied by these calculations.

Attempts to include sizable electron–electron interactions within an itinerant electron theory are based on the partial summation of ladder and bubble diagrams, in the spirit of Eq. (1). This leads to the RPA type theory of Ref. [40–43] and the fluctuation exchange approximation of multiband systems [44,45]. RPA calculations yield a magnetic susceptibility that is peaked at or near $\mathbf{Q}=(\pi,\pi)$. For parameters where the Fermi surface around Γ is present, the dominant pairing channel is again the $s^{\pm}$-state, while d-wave pairing occurs as one artificially eliminates this sheet of the Fermi surface. The exchange of paramagnons between Fermi surface sheets is shown to be an efficient mechanism for spin fluctuation induced pairing. The fluctuation exchange (FLEX) approach is to some extent a self consistent version of the RPA theory [46]. While the method is not very reliable to address high energy features, the description of the low energy dynamic spin response, the low energy electronic band renormalization and the nature of the pairing instability are rather reliable. The fact that several orbitals matter in the FeAs systems is also of help as FLEX type approaches can be formulated as theories that become exact in the limit of large number of fermion flavors [47]. Refs. [44,45] performed FLEX calculations for the FeAs systems and find once again that the dominant pairing state is an $s^{\pm}$-state, even though Ref. [44] also find a d-wave state in a regime where the magnetic fluctuation spectrum is peaked at vectors away from $\mathbf{Q}=(\pi,\pi)$. These authors find a solution that is numerically close to a compact form

$$\Delta(\mathbf{k}) = \Delta_0\cos(ak_x)\cos(ak_y), \qquad (3)$$

but this form is neither required by symmetry nor can be consistently deduced from any low-energy theory (where pairing occurs at or near the Fermi surface). We will come back to this issue later in this review.

To summarize, numerous calculations that start from an itinerant description of the magnetic interactions yield an $s^{\pm}$ pairing state caused by the exchange of collective interband scattering or paramagnons.

2.2.4. J_1–J_2 model

The initially assumed absence of the Drude weight in undoped ferropnictides has been taken as evidence for the fact that they are in the vicinity of a Mott transition and should be considered as bad metals with significant incoherent excitations [48]. Subsequent experiments [49] observed however a Drude weight, as expected for an almost semi metal. In case of an absent or anomalously small Drude weight, it is clearly appropriate to start from a theory of localized spins, analogous to what is believed to be correct in the cuprate superconductors [50,51]. It is worth noting that proximity to a Mott transition is a sufficient, but not necessary condition for existence of local moments. If the dominant magnetic interactions are between nearest and next-nearest-neighbor Fe-spins, the following model describes the localized spins:

$$H = J_1\sum_{\langle i,j\rangle}\mathbf{S}_i\cdot\mathbf{S}_j + J_2\sum_{\langle\langle i,j\rangle\rangle}\mathbf{S}_i\cdot\mathbf{S}_j \qquad (4)$$

Here, J_1 and J_2 are the superexchange interactions between two nearest-neighbor and next-nearest-neighbor Fe sites, respectively. A geometrical argument can be made [52,48] that indeed the two superexchange paths *via* As have comparable strength (however, this argument fails to recognize that the direct overlap between Fe orbitals in pnictides is very large [53], thus leading to a strong enhancement of the nearest neighbor antiferromagnetic exchange in the localized picture [54], and that the classical Anderson-Kanamori superexchange is only operative if the band widths are smaller than the Hubbard U, which is not the case is ferropnictides). When $J_1 > 2J_2$ the conventional Neel state has the lowest energy, when $J_1 < 2J_2$ the stripe order emerging in the experiment is the lowest magnetic state. The system is frustrated if $J_1 = 2J_2$.

Upon doping the poor metal (strictly the insulator) described by Eq. (4) with charge carriers can be investigated for superconductivity, with pairing stabilized by strong quantum spin fluctuations. In Ref. [55] a single band of carriers was investigated leading to either $d_{x^2-y^2} + id_{xy}$ or d_{xy}-pairing, depending on the carrier concentration and the precise ratio of J_1 and J_2. A more realistic theory for the pairing in the J_1-J_2 model in the pnictides must of course include at least two bands and was developed in Ref. [56]. For sufficiently large J_2, the $s^{\pm}$-state is once again the dominating pairing state. It may seem strange that this strong coupling theory based upon the assumption of a proximity to a Mott transition (regardless of the fact the experiments so far have not supported this assumption) has essentially the same pairing solutions (d-wave for one Fermi surface sheet and $s^{\pm}$-wave for two Fermi surface sheets separated by $\mathbf{Q}$), as the RPA calculation [40]. In Section 3 we will explain that this is not surprising at all and that even a totally unphysical theory may lead to perfectly sensible results for superconductivity, as long as it has the same structure of magnetic excitations in the reciprocal space.

2.3. Magneto-elastic coupling

The parent compounds exhibit a structural and a magnetic transition, strongly suggesting that magneto-elastic coupling plays a role in the physics of pnictides in general and in superconductivity in particular. Electronic structure calculations for a nonmagnetic state indicate that the electron–phonon interaction in the pnictides is rather modest and definitely not sufficient to explain superconducting transition temperatures of 50 K [57,5]. However, as these calculations were based on the nonmagnetic electronic structure, effects of local magnetism on iron were entirely neglected. Indeed, the equilibrium position of As calculated under this assumption are quite incorrect and the force constant for the Fe–As bond is 30% higher than it should be. On the other hand, fully magnetic AFM calculations, while overestimating the ordered moment, produce highly accurate equilibrium structures and the force constant in agreement with experiment [22] (a detailed discussion can be found in T. Yildirim's contribution to this volume). It was pointed out that including soft magnetism in the calculation, i.e. magnetism with directional and amplitude fluctuations, may substantially enhance the electron–phonon coupling [58]. The emphasis is on "soft": additional reduction of the force constants of the Fe–As bonds does not come from the fact that the moment exists, but from the fact that the amplitude of the moment depends on the bond length. Intriguingly, in the 1111 systems the AFM transition occurs somewhat below a structural phase transition. Both transitions seem to be of the second order, or of very weakly first order [23]. In undoped 122 compounds the structural and magnetic orders emerge simultaneously through a strong first order transition [59,60].

In the ordered state, Fe-spins are parallel along one direction and antiparallel along the other. Since we expect the bond length for parallel and antiparallel Fe-spin polarization to be distinct, magnetism couples strongly to the shear strain $\varepsilon_{\rm shear} = \varepsilon_{xy} - \varepsilon_{yx}$. Thus, $\varepsilon_{\rm shear} \neq 0$ should invariably occur below the Neel temperature. Experiment finds that the ferromagnetic bonds are shorter than antiferromagnetic bonds. From the point of view of superexchange interaction it seems somewhat surprising that ferromagnetic bonds shorten and the superexchange-satisfied bonds expand. Yet this behavior is exactly the same as the DFT calculations had predicted [52], and it can be traced down to one-electron energy (the observed sign of the orthorhombic distortion simply lowers the one-electron DOS at the Fermi level) [100].

What remains puzzling is however why in the 1111 family the structural transition occurs above T_N. Naively, this fact could be taken as evidence for a hypothesis that elastic degrees of freedom are

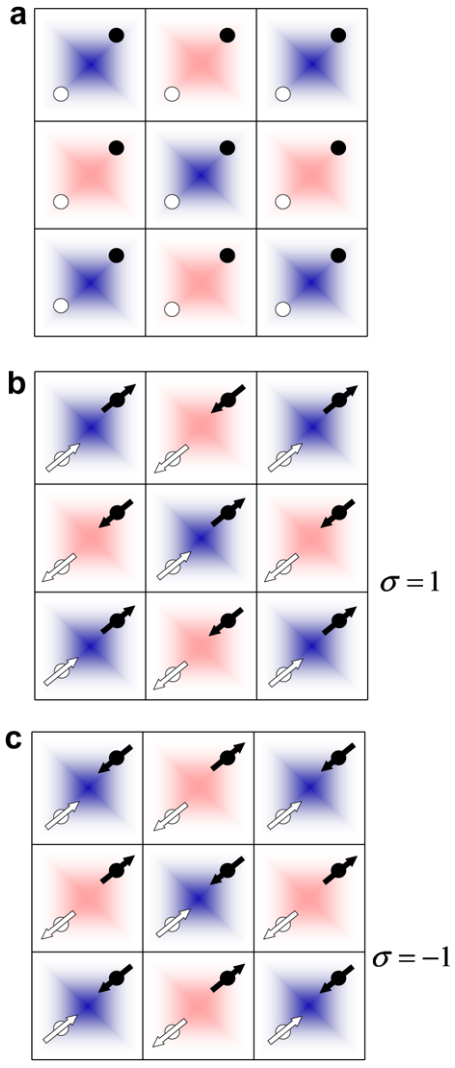

Fig. 7. (a) Fe_2 lattice with the fully symmetric unit cells shown. The full circles denote one sublattice, the hollow ones the other. Shading shows ordering corresponding to the vector $\mathbf{Q} = (\pi, \pi)$ in the Fe_2 lattice; for each sublattice, spins in the pink unit cells are opposite to the spins in the blue cells, but relative orientation of the two sublattices is arbitrary. (b) Ordered state with $\mathbf{Q} = (\pi, \pi)$ and with parallel orientation of the spins in the unit cell ($\sigma = 1$). (c) Same ordering vector $\mathbf{Q} = (\pi, \pi)$, but with antiparallel orientation of the spins in the unit cell ($\sigma = -1$).

the driving force and that magnetism is secondary. There are strong quantitative and qualitative arguments against this view. First, numerous DFT calculations [61,62,22] converge to the correct orthorhombic structure (with correct sign and magnitude of the distortion), if performed with AFM magnetic ordering, and to a tetragonal solution if done without magnetism. On the other hand, the antiferromagnetism is obtained even without allowing for a structural distortion. In other words, magnetism is essential for the distortion, but the distortion is not needed for the magnetism.

There exists also a very general argument that demonstrates that the magnetism is indeed primary and the structural distortion secondary. Historically the relevant physics was first encountered in the 2D J_1-J_2 model [63], and applied to ferropnictides in Refs. [50,51]. Below we will reformulate this argument from a general point of view. We begin with a unit cell that contains two Fe sites (just as the actual crystallographic unit cell for the FeAs trilayer). The most natural choice of the origin is in the middle between these two Fe cites (Fig. 7a). The coordinates of the atoms are

$\mathbf{r}_{ij}^{+} = \mathbf{R}_{ij} + \mathbf{d}, \mathbf{r}_{ij}^{-} = \mathbf{R}_{ij} - \mathbf{d}, \mathbf{d} = (\frac{1}{4}, \frac{1}{4})$, where $\mathbf{R}_{ij}$ (ij integer) are the coordinates of the centers of the unit cells. This naturally implies partitioning the entire lattice into two sublattices, shown as open and solid dots in Fig. 7a.

Both ferro- and checkerboard antiferromagnetic orderings correspond to a $\mathbf{Q} = (0,0)$ perturbation of the uniform state, since in both cases all unit cells remain identical. The Fourier transform of either pattern contains only momenta corresponding to the reciprocal lattice vectors. Conversely, a spin-density wave with the quasi-momentum $\mathbf{Q} = (\pi,\pi)$ corresponds to flipping all spins in every other unit cell, as illustrated in Fig. 7b and c by shading colors (blue cells have the magnetization density opposite to that of the pink cells). It is evident from Fig. 7b and c that this imposes no requirement upon the mutual orientation of the two sublattices. Again, one can say that the susceptibility as a function of *quasi*-momentum **q** inside the first Brillouin zone does not describe fluctuations of the magnetic moment of two ions in the same unit cell with respect to each other, for that purpose one needs to know the linear response at all momenta **q+G**, where **G** is an arbitrary reciprocal lattice vector.

Let us assume that the most stable mean-field phase corresponds to Néel order in each of the two sublattices. In the J_1–J_2 language that corresponds to $J_2 > J_1/2$, in the itinerant language to an instability in χ at $\mathbf{Q} = (\pi,\pi)$. Moreover, it is obvious from Fig. 7b and c that in the classical ground state one sublattice does not exchange-couple at all to the other, so the classical ground state is infinitely degenerate. This is however not important for the following discussion, what matters is that the two extreme cases are always degenerate, the one where two spin in the same cell are parallel (Fig. 7b) or antiparallel (Fig. 7c). In the $J_1 + J_2$ model the infinite degeneracy is reduced by quantum fluctuations, but the double degeneracy remains, while in the LDA it is only double degenerate already on the mean-field level [64].

It is instructive [63] to introduce two order parameters corresponding to the Neel (checkerboard) ordering for each sublattice, $\mathbf{m}_{\pm} = \sum_{ij}(-1)^{i+j}\mathbf{M}_{ij}^{\pm}$, where $\mathbf{M}_{ij}^{\pm}$ are the magnetic moments of the two Fe's in the unit cell ij. Following Ref. [63] one can introduce the third (scalar) order parameter, $\sigma = \sum_{ij}\sigma_{ij} = \sum_{ij}\mathbf{M}_{ij}^{+}\cdot\mathbf{M}_{ij}^{-}$. Now $\sigma > 0$ corresponds to parallel orientation of the magnetization inside the unit cell (Fig. 7b) while $\sigma < 0$ refers to antiparallel orientation (Fig. 7c). In the former case $\sigma > 0$, neighboring Fe-spins are parallel along the diagonal and antiparallel along the counter-diagonal. The situation is reversed for $\sigma < 0$. These two configurations are degenerate and correspond to the frequently discussed 'stripe' magnetic order. In two dimensions, according to the Mermin–Wagner theorem, σ is the only order parameter that can be finite at finite temperature. Therefore the presumably largest energy scale of the system, the mean-field transition temperature of each sublattice, T^* ($\sim J_2$ in the local model, and the energy difference E_{FM}–E_{AFM} in the itinerant picture), does not generate any phase transition, but rather starts a crossover regime where the correlation length ξ_m for the $\mathbf{m}_{\pm}$ order parameter becomes much longer that the lattice parameter.

In this regime, one can investigate a possibility of a phase transition corresponding to the σ order parameter. It is important to realize that σ does not have to change sign along a domain wall of the magnetization. This ensures that σ can order even though the sublattice magnetization vanishes. σ does couple to the (long-range) fluctuations of **m**; integrating these fluctuations out one will obtain an effective Hamiltonian coupling σ_{ij} and $\sigma_{i'j'}$ as far as ξ_m, meaning that even very small coupling between $\mathbf{m}_+$ and $\mathbf{m}_-$ will produce a phase transition to a finite σ at a temperature $T_s \sim J_1\xi_m^2(T_s) \sim J_1\exp(J_2/T_s)$. Solving this for T_s, one gets $T_S \sim J_2/\log(J_2/J_1)$. Note that here again J_1 and $J_2 \sim T^*$ just characterize the relevant energy scales and by no means require the validity of the $J_1 + J_2$ model.

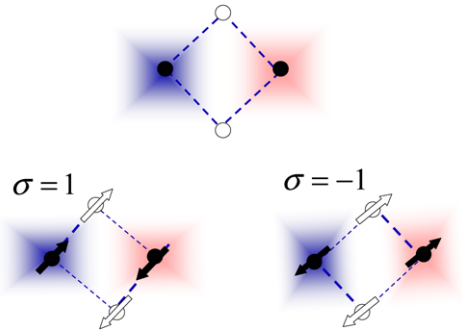

Fig. 8. Magneto-elastic coupling: the two atoms per unit cell are denoted by filled and open circles. A ferromagnetic bond leads to a shortening of the nearest neighbor lattice constant (bold dashed lines), while an antiferromagnetic bond leads to a longer lattice constant (thin dashed lines). Depending on the relative orientation of the two sublattices (i.e. the sign of σ), two distortions with opposite sign of $\varepsilon_{\text{shear}}$ are possible.

As mentioned above σ is positive (negative) for ferromagnetic (antiferromagnetic) bonds, see Fig. 8. Thus σ couples bilinearly to the order parameter of the orthorhombic structural transition

$$F_c = \gamma\varepsilon_{\text{shear}}\sigma. \tag{5}$$

When the expectation value of σ is nonzero below a transition temperature T_s, the tetragonal symmetry is spontaneously broken leading to $\varepsilon_{\text{shear}} \neq 0$. We see that T_s is suppressed from T^* rather weakly (logarithmically) and that even a weak coupling between the two sublattices would produce a structural phase transition.

The third energy scale existing in the problem is set by the interlayer magnetic coupling, $J_\perp$. In the DFT we found $J_\perp \lesssim 1$ meV in LaFeAsO and $J_\perp \sim$ 6 meV in $BaFe_2As_2$ [4]. This huge difference defines the different behavior of these two compounds. In the former the Neel transition temperature for a sublattice ordering is on the order of $T^*/\log(T^*/J_\perp)$, logarithmically smaller than T_s, while in the latter one expects a much larger T_N, and likely larger than the T_s for an individual FeAs plane.

The phase between T_N and T_s, if $T_s > T_N$, was dubbed "nematic" in Refs. [50,51], as the order parameter $\langle\sigma\rangle \neq 0$ even though $\langle\mathbf{M}_{ij}\rangle = 0$, as expected for an axial, as opposed to vectorial order parameter. The first order nature of the transition in the 122 systems is then likely a consequence of the coupling to soft elastic degrees of freedom, and/or of nonlinear interactions. A more rigorous treatment of the described physics will be published elsewhere [65]. There is another interesting experimental evidence for the unconventional nature of the magneto-elastic coupling in these systems. In the 122 systems the structural distortion $\propto\varepsilon_{\text{shear}}$ and the sublattice magnetization seem to be proportional to each other. [66] At a second order transition, symmetry arguments imply however that the former should be proportional to the square of the sublattice magnetization. At a first order transition, no such strict connection can be established, however one expects that the generic behavior is recovered as the strength of the first order transition gets smaller, realizable via alkaline earth substitution. Experiments show that the mentioned linear behavior is similar for Ca, Ba or Sr [67]. Arguments that the first order character of the magneto-elastic phase transition originates from the lattice instabilities near the onset of spin-density wave order were recently given in Ref. [68]. However, further discussion clearly goes beyond the limit of this review.

The fact that at the structural transition (and even above), magnetic correlations in plane are already well established, with large correlation lengths, explains many otherwise mysterious observations. A more detailed discussion can be found in Ref. [22].

This picture is not without ramifications for superconductivity. First and foremost, it implies that at superconducting composition

ferropnictides, especially the 1111 family, are not really paramagnetic, bat rather systems with a large in-plane magnetic correlation length, much larger than the lattice parameter and likely much larger than the superconducting correlation length. Second, the excitation structure in such a system is unusual and cannot be entirely described in terms of $\chi(\mathbf{Q})$, where $\mathbf{Q}=(\pi,\pi)$, since such a description loses the physics associated with the parameter σ. Finally, it implies that the lattice and spin degrees of freedom do not fluctuate independently and are naturally connected to each other. Therefore a detailed quantitative theory for the pairing state will have to include lattice vibrations. Conversely, experiments that find evidence for a lattice contribution to the pairing mechanism should not be considered as evidence against magnetic pairing.

2.4. Other excitations

While everybody's attention is attracted to magnetic pairing mechanisms and spin fluctuations, it would be premature and preposterous to exclude any other excitations from consideration. First of all, it might be still too early to discard the venerable phonons. While there is no question that the calculations performed so far [57,5] were accurate and the linear response technique used had proved very reliable before (MgB_2, CaC_6, *etc.*), these calculation by definition do not take into account any effects of the magnetism. As discussed above, it is very likely that the ground state even in the so-called nonmagnetic region of the phase diagram is characterized by an AFM correlation length long enough compared to the inverse Fermi vector. In this case, the amplitude of the magnetic moment of Fe (even though its direction fluctuates in time) is nonzero and the electronic structure is sensitive to it. Calculations suggest that a phonon stretching the Fe–As bond will strongly modulate this magnetic moment and thus affect the electronic structure at the Fermi level more than for a nonmagnetic compound (or, for that matter, a magnetic compound with a hard magnetic moment). Softness of the Fe moments, variationally, provides an additional route for electron–phonon coupling and should therefore always enhance the overall coupling constant. Whether this is a weak or a strong effect, and whether the resulting coupling is stronger in the intraband channel (enhancing the $s_{\pm}$ superconductivity) or in the interband channel (with the opposite effect), is an open question. Only preliminary results are available [58].

Besides the phonons and the spin fluctuation, charge (polarization) fluctuations can also, in principle, be pairing agents. To the great surprise of the current authors, nobody has yet suggested an acoustic plasmon mechanism for ferropnictides, a mechanism that was unsuccessfully proposed for cuprates, for MgB_2 and for CaC_6. Presumably the apparent lack of strong transport anisotropy in 122 and the absence of carriers with largely disparate mass prevented these usual suspects from being discussed.

It is not only the harsh condition on the very existence of acoustic plasmons, but a very general malady (better known in the case of acoustic plasmons, but generally existing for any sort of exciton pairing) that prevents plasmonic superconductivity in most realistic cases: lattice stability. Basically, efficient pairing of electrons via charge excitations of electronic origin requires overscreening of electrostatic repulsion—which by itself does not constitute a problem. But since the ion–ion interaction is screened by the same polarization operator as electron–electron interaction, there is an imminent danger that the former is overscreened as well. This is an oversimplified picture (electron–electron susceptibility differs from the response to an external field on the level of vertex corrections), but it captures the essential physics [102].

This danger was appreciated by the early proponents of the excitonic superconductivity, Little [69] and Ginzburg [70], therefore they proposed space separation between a highly polarizable insulating media, providing excitons, and a metallic layer or string where the superconducting electrons live. The sandwich structure of the As–Fe–As trilayer reminds us of the Ginzburg's "sandwich" ("Ginzburger") and tempts to revisit his old proposal.

This was done recently by Sawatzky and collaborators [71] who pointed out that As is a large ion (Pauling radius for As^{4-} is 2.2 Å) and ionic polarizability grows with the radius cube. Since the conducting electrons are predominantly of Fe origin, they suggested pairing of Fe d electrons *via* polarization of As ions. So far, this proposal was received with a skepticism that can be summarized as follows. (1) Analyzing the muffin-tin projected character of the valence bands, as it was done in Ref. [71], is generally considered to be an unreliable way to estimate the hybridization between different ions; indeed the largest part of the electronic wave function refers to the interstitial space, which is naturally identified as mostly As-like. (2) Removal of the As orbitals from the basis leads to a strong reduction of the valence band width, indicating that hybridization between Fe and As is about as strong as direct Fe–Fe hopping. (3) When Bloch functions are projected upon the Fe-only Wannier functions, the latter come out very diffuse and extend way beyond the Fe ionic radius. That is to say, negligible hybridization between Fe and As, that is prerequisite for the scenario promoted in Ref. [71], appears to be a rather questionable proposition. Besides, above-mentioned calculations of the phonon spectra and electron–phonon coupling implicitly account for the large susceptibility of the As^{-4} ions (which comes mostly from the outer, valence shell) yet they find no manifestation of strong As polarization: neither particular phonon softening nor strong coupling with any phonon.

3. Pairing symmetry: general considerations

3.1. Geometrical consideration: excitation vectors and Fermi surface

Given such disparate views that different researchers hold about the origin of magnetism in ferropnictides and of the character of spin fluctuations there, it may seem strange that a great majority of model calculations predict the same pairing symmetry, $s_{\pm}$, with full gaps in both electron and hole bands, but with the opposite signs of the order parameters between the two. In fact, this is not surprising at all. To begin with, let us point out that the sign of the interaction mediated by boson exchange is always positive (attraction) for charge excitations (phonons, plasmons, polarization excitons), since the components of a Cooper pair have the same charge, but can be either positive (for triplet pairing, where the electrons in the pair have the same spin) or negative (repulsion) for singlet pairing, for spin excitations. That is to say, exchange of spin fluctuations mediates repulsion. A quick glance at the anisotropic BCS equation reveals that repulsive interactions can be pairing when, and only when the wave vector of such a fluctuation spans parts of the Fermi surface(s) with opposite signs of the order parameter (equivalently, one can say that an interaction that is repulsive everywhere in the momentum space, can be partially attractive in the real space, for instance, for electrons located an nearest lattice sites).

This can be illustrated by a popular model of high-T_c cuprates, which considers a simplified cylindrical Fermi surface nearly touching the edge of the Brillouin zone and superexchange-driven spin fluctuations with the wave vector (π,π). As Fig. 9a illustrates, such an interaction is pairing in the $d_{x^2-y^2}$ symmetry, because it spans nearly perfectly the lobes of the order parameter with the opposite signs.

Most models used for ferropnictides assume a simplified fermiology with one or more hole FSs and one or more electron FSs displaced by the SDW vector $(\pi,0)$ (in this section, we use the notations corresponding to the Brillouin zone with one Fe per cell).

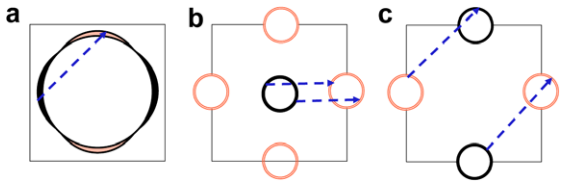

Fig. 9. (a) A cartoon illustrating how a repulsive interaction corresponding to superexchange spin fluctuations $\mathbf{Q}=(\pi,\pi)$ may generate d-wave pairing in cuprates. (b) The same, for an $s_\pm$ state and spin fluctuations with $\mathbf{Q}=(\pi,0)$ (in a Brillouin zone corresponding to one Fe per cell). (c) If the central hole pocket is absent, the superexchange interaction favors a nodeless d state. Here the pink color indicates a positive order parameter, and the black color the negative one. (For interpretation of the references to color in this figure legend, the reader is referred to the web version of this article.)

Any spin-fluctuation induced interaction with this wave vector, no matter what the origin of these fluctuations (FS nesting, frustrated superexchange, or anything else) unavoidably leads to a superconducting state with the opposite signs of the order parameter for the electrons and for the holes. Depending on the details of the model the ground state maybe isotropic or anisotropic and the gap magnitudes on the different sheets may be the same or may be different, but the general extended s symmetry with the sign-reversal of the order parameter (an $s_\pm$ state) is predetermined by the fermiology and the spin fluctuation wave vector (Fig. 9b).

It is worth noting that while most (but not all) models consider spin fluctuations corresponding to the observed instability to be the leading pairing agent, some include spin fluctuations of different nature [for instance, nearest neighbor superexchange or nesting between the "X" and "Y" electron pockets, both corresponding to the same wave vector, (π,π) in the unfolded zone and (0,0) in the conventional zone], or phonons, or direct Coulomb repulsion; these additional interactions may modify the gap ratios and anisotropies (in extreme cases, creating nodes on some surfaces), but, for a realistic choice of parameters, unlikely to change the symmetry.

Moreover, if the radius of the largest FS pocket is larger than the magnetic vector, spin fluctuations start to generate an *intraband* pair-breaking interaction, which by itself will lead to an angular anisotropy and possible gap nodes.

The above reasoning, however, is heavily relying upon an assumption that the topology predicted by the DFT is correct. So far, as discussed above, the evidence from ARPES and from quantum oscillations has been favorable. It is still of interest to imagine, for instance, electron-doped compounds not having hole pockets at all or having them so small that the pairing energy for them is negligible. It was pointed out [40,72] that in this case spin fluctuations with different momentum vectors dominate and create a nodeless d-wave state in the electron pockets, as Fig. 9c illustrates.

3.2. General properties of the $s_\pm$ state

Since the $s_\pm$ states constitute the most popular candidate for the superconducting symmetry of pnictides, it is worth recapitulating the physics of this state. Let us start with the simplest possible case: two bands (two Fermi surfaces) and interband repulsive interaction between the two. Let the interaction strength be $-V$, and the DOSs $N_1 \neq N_2$. To be specific, let $N_2 = \alpha N_1, \alpha \geqslant 1$. Then in the weak-coupling limit the BCS equations read

$$\Delta_1 = -\int d\epsilon \frac{N_2 V \Delta_2 \tanh(E_2/2k_BT)}{2E_2}$$
$$\Delta_2 = -\int d\epsilon \frac{N_1 V \Delta_1 \tanh(E_1/2k_BT)}{2E_1} \quad (6)$$

where E_i is the usual quasiparticle energy in band i given by $\sqrt{(\epsilon-\mu)^2+\Delta_i^2}$. Near T_c linearization gives

$$\Delta_1 = \Delta_2 \lambda_{12} \log(1.136\omega_c/T_c)$$
$$\Delta_2 = \Delta_1 \lambda_{21} \log(1.136\omega_c/T_c), \quad (7)$$

where $\lambda_{12} = N_2 V$, the dimensionless coupling constant, with a similar expression for λ_{21}. These equations readily yield $\lambda_{eff} = \sqrt{\lambda_{12}\lambda_{21}}$ and $-\Delta_1/\Delta_2 = \sqrt{N_2/N_1} \equiv \sqrt{\alpha}$. Note that the Fermi surface with the larger DOS has a smaller gap. It can also be shown [103] that the gap ratio at zero temperature in the weak-coupling limit is also given by $\sqrt{N_2/N_1}$, and strong coupling effects tend to reduce the disparity between the gaps.

The situation becomes more interesting for more than two orbitals with distinct gaps. Let us consider a model for the hole-doped 122 compound. The calculated FS (Fig. 4) shows three sets of sheets: Two e-pockets at the corner of the zone, two outer h-pockets, formed by the xz and yz orbitals (degenerate at Γ without the spin-orbit), and the inner pocket formed by x^2-y^2. In the DFT calculations all three hole cylinders are accidentally close to each other, however, ARPES shows two distinct sets, the inner barrel, one of which presumably corresponding to x^2-y^2 band, and the outer one, presumably xz/yz. The pairing interaction between the e-pockets and the two different types of the h-pockets need not be the same (by virtue of the matrix elements). Using the same partial DOS as listed above for $Ba_{1.6}K_{0.6}Fe_2As_2$ (both total and individual DOS depend weakly on the position of the Fermi level, reflecting the 2D character of the band structure at this doping), roughly 1.2 st/eV for each hole band and the same for the two e-band together, we get the coupling matrix

$$\begin{pmatrix} 0 & 0 & -\lambda_1\nu_1 \\ 0 & 0 & -\lambda_2\nu_2 \\ -\lambda_1 & -\lambda_2 & 0 \end{pmatrix}, \quad (8)$$

where $\nu_{1,2}$ is the ratio of DOS of the first (xz/yz) and the second (x^2-y^2) hole bands to that of the electron bands. Note that $\nu_1 \sim 2$ and $\nu_2 \sim 1$. Diagonalizing this matrix we find the gap ratios to be $\Delta_1 : \Delta_2 : \Delta_e = \lambda_1 : \lambda_2 : \sqrt{\lambda_1^2\nu_1 + \lambda_2^2\nu_2}$. The latest ARPES measurements [11] imply that $\Delta_i{:}\Delta_o \approx 2{:}1$, where i and o stand for the inner and outer sets of hole Fermi surfaces. This would mean that the two coupling constants are twice larger that the other (although we do not know which), which is fairly possible. However, that implies that the electron FS has a gap that is larger than that of the largest hole band by at least a factor of $\sqrt{1.5} = 1.22$ (assuming that the outer FSs in the calculations, are formed by the xz/yz bands; the opposite assumptions leads to an even larger electron-band gap). This is in some disagreement with the ARPES data that suggest that Δ_e is on the order of Δ_i or slightly smaller. However, this is a small discrepancy, which can be easily corrected by introducing small intraband electron–phonon coupling for the hole bands, and/or taking into account possible gap suppression by impurities in the electron band. It is also worth noting that the spread of the measured values, depending on the sample and on the location on the FS, is on the order of 10%.

3.3. Coulomb avoidance

It was realized quite some time ago that a d-wave pairing has an additional advantage compared to an s-wave, namely that the electrons in a Cooper pair avoid each other (the pair wave function has zero amplitude at $\mathbf{r}-\mathbf{r}' = 0$), strongly reducing their local Coulomb repulsion. The leading contribution to the pairing interaction in the single band Hubbard model $U\Sigma_{\mathbf{k}}\langle c_{\mathbf{k}\uparrow}c_{-\mathbf{k}\downarrow}\rangle$ is repulsive, but vanishes as $\Sigma_{\mathbf{k}}\Delta_{\mathbf{k}} = 0$ due to the symmetry of the d-wave state.

Thus, a contact Coulomb repulsion does not affect d-wave superconductivity.

The simplest possible $s^{\pm}$-wave function is given by Eq. (3). In this case, the sum over the Brillouin zone vanishes again due to nodes at $\pm ak_x \pm ak_y = \pi/2$. This description is however somewhat misleading because it may produce a false impression that there is a symmetry reason for the vanishing of the Coulomb repulsion in the $s^{\pm}$ state, or that this particular functional form is essential for avoiding the Coulomb repulsion. To illustrate that this is not the case, it is instructive to consider a toy problem in reciprocal space. In the weak-coupling regime, the effective coupling matrix $\Lambda_{\mathbf{k}\mathbf{k}'}$ (note that the band index is uniquely defined by the wave vector) is

$$\Lambda_{\mathbf{k}\mathbf{k}'} = \lambda_{\mathbf{k}\mathbf{k}'} - \mu^*_{\mathbf{k}\mathbf{k}'}, \tag{9}$$

where λ is the original coupling matrix in orbital space and $\mu^*_{\mathbf{k}\mathbf{k}'}$ is the renormalized Coulomb pseudopotential. The critical temperature is determined by the largest eigenvalue of the matrix Λ, and the $\mathbf{k}$ dependence of the order parameter $\Delta_{\mathbf{k}}$ is given by the corresponding eigenvector. If μ^* is a constant and $\Sigma_{\mathbf{k}}\Delta_{\mathbf{k}} = 0$ (as in the d-wave case), any eigenvector of the matrix λ is also an eigenvector of Λ, with the same eigenvalue. This proves that Coulomb avoidance takes place for any superconductor where the order parameter averages to zero over the entire FS, and not only for the d-wave symmetry.

Let us now consider a specific $s^{\pm}$ superconductor. For simplicity, let us take two bands with the same DOS, $N_1 = N_2 = N$ and with an interband coupling only:

$$\lambda_{ij} = \begin{pmatrix} 0 & -VN \\ -VN & 0 \end{pmatrix}. \tag{10}$$

We shall also assume that the Coulomb repulsion U is a contact interaction, so that $\mu^*_{ij} = UN$ is the same for all matrix elements. The maximal eigenvalue of Λ, which corresponds to the effective coupling constant λ_{eff}, is indeed simply VN and *independent* of U. The corresponding eigenvector is $\Delta_1 = -\Delta_2$, i.e. the $s^{\pm}$ state. The Coulomb interaction is irrelevant, just like in case of d-wave pairing. The effect is however a consequence of the assumed symmetry of the two bands. In general, unlike d-wave pairing, no symmetry requires that $\Sigma_{\mathbf{k}}\Delta_{\mathbf{k}} = 0$. This can already be seen if one considers a model with distinct densities of states: $N_2 = \alpha\ N_1 = \alpha N$. We have

$$\lambda_{ij} = \begin{pmatrix} 0 & -\alpha VN \\ -VN & 0 \end{pmatrix}. \tag{11}$$

and the weak-coupling gap ratio near T_c is $\sqrt{\alpha}$. Now the effect of the Coulomb repulsion is not nullified, but is still strongly suppressed. The eigenvalues are easily determined. The key result is that the maximal eigenvalue remains positive for all finite α. Even the extreme limit $\lambda^{\pm}_{\text{eff}}(U \to \infty) = 2VN\alpha/(1+\alpha)$ is for realistic α only somewhat reduced compared to $\lambda^{\pm}_{\text{eff}}(U = 0) = \sqrt{\alpha}VN$. This is qualitatively different from the regular (s_{++}) interband-only pairing with an attractive interband interaction of the same strength. In this case, $\lambda^{++}_{\text{eff}}(U > V/2) < 0$, and the Coulomb interaction dominates over the attractive interband pairing interaction. In the linear in UN regime, the suppression rate of $\lambda_{eff}(U)$ is $(\sqrt{\alpha}-1)/2$ for $s^{\pm}$ and $(\sqrt{\alpha}+1)/2$ for s^{++} pairing. For example, for the DOSs ratio of 4 (the gap ratio is then 2) $\mu^* \approx 0.25\lambda_{eff}(U = 0)$ will suppress an s^{++} superconductivity entirely, while in the $s^{\pm}$ case the effective coupling will be reduced only by 8%.

The efficiency of the Coulomb avoidance is neither limited to the assumption of a uniform Coulomb interaction among and within the bands, nor is a result of the weak-coupling approach. Strong coupling FLEX type calculations also find pairing states with very small repulsive contribution due to Coulomb interaction [44,45].

4. Pairing symmetry: experimental manifestations

4.1. Parity

Since we want to review the experimental situation regarding the pairing symmetry, the first question to ask is, whether superconductivity is singlet or triplet? Fortunately, this question can be answered relatively confidently. Measurements of the Knight shift on single crystals of the Co-doped $BaFe_2As_2$ superconductor [73] clearly indicate full suppression of spin susceptibility in the superconducting state *in all directions*, incompatible with a triplet pairing in a tetragonal crystal. For other compounds only polycrystalline, direction-averaged data exist, but they fully agree with the above result, virtually excluding triplet superconductivity. This leaves, of all possible scenarios, essentially three: conventional s (presumably multi-gap), $s_{\pm}$ and d.

4.2. Gap amplitude

All experiments that distinguish between different pairing states can be, roughly speaking, grouped into two classes: those probing the gap amplitude and those probing the gap symmetry. The advantage of the former is that they are comparatively easier to perform. The temperature dependence of any observable sensitive to the excitation gap is sensitive to the presence of nodes or multiple gaps. The disadvantage is that only a measurement of the relative phase of the wave function will unambiguously determine the pairing state, including its symmetry.

Important and very transparent probes of the gap amplitude are thermodynamic measurements. The early reports of the specific heat leaned towards power-law behavior characteristic of nodal superconductivity. The latest data [13,15] suggest a fully gapped superconductivity, or a dominant fully gapped component with possible small admixture of a nodal state. While the experimental situation is still far from being in consensus, especially regarding the 1111 family, a few observations may be in place: (i) The specific heat jump in the h-doped $BaFe_2As_2$ is strong and sharp, and in the 1111 compounds is weak and poorly expressed. This cannot be ascribed to a difference in calculated band structures. This is either due to sample quality issues or possibly to the more isotropic character of superconducting and magnetic properties in 122 systems. (ii) In no case the specific heat temperature dependence be fitted with one gap. Multiple gap fits, having more parameters, are of course less reliable. (iii) Another, usually more reliable signature of nodal superconductivity is a square-root dependence of the specific heat coefficient on the magnetic field. Existing reports [13] however show a clear linear dependence, characteristic of a fully gapped superconductor.

Another popular probe is temperature dependence of the NMR relaxation rate. Extensive studies have been done in this aspect (see other articles in this volume). In all studied systems, the relaxation rate is non-exponential. The initial impression was that the relaxation rate is cubic in temperature, $1/T_1 \propto T^3$, consistent with nodal lines [74,75]. Later it was argued that the data cannot be described by a single power law as in the cuprates [76,77]. These results were obtained for the 1111 systems. The situation with the 122 family is even less clear. Published data [78,73] do not show exponential decay either, but the results are equally far from any single power law behavior. Even more puzzling, the only paper reporting on the low-T_c LaFePO superconductor claims that the relaxation rate does not decrease below T_c at all [79].

The third relevant experiment is measuring the London penetration depth. Reports are again contradictory. For instance, in Pr-based 1111 compound the penetration depth was found [80] to barely change between $\approx 0.05T_c$ and $T^* \approx 0.35T_c$, and than in-

crease roughly as $(T-T^*)^2$ between T^* and $\approx 0.65T_c$, a picture roughly consistent with a multi-gap nodeless superconductor. Malone *et al* [81] measured Sm-based 1111 and were able to fit their data very well in the entire interval from $T_c/30$ and T_c using two full gaps. In Nd-based 1111 the penetration depth was measured at $T > 0.1T_c$ and fitted with a single anisotropic gap for $0.1T_c < T < T_c/3$, [82] however, the latest result from the same authors, taken at lower temperature, can be better fitted with a quadratic law [83]. Similar quadratic behavior has been clearly seen in the 122 compounds [84]. At the same time, the low-T_c LaFePO is again odd: it shows a linear behavior [85].

To summarize, the thermodynamic data on average lean towards a nodal superconductivity. However, *some* data are not consistent with the gap nodes, and there is no clear correlation with the sample quality either way. Moreover, while some data suggest line nodes, others are consistent only with point nodes, in the clean limit. One can say with a reasonable degree of confidence that the entire corpus of the data cannot be described by any one scenario in the clean limit. On the other hand, essentially any temperature dependence of thermodynamic characteristics can be fitted if a particular distribution of impurity scattering is assumed in an intermediate regime between the Born and the unitary scattering, and a particular relation between the intra- and interband scattering (there have been a number of paper doing exactly that for the NMR relaxation rate, for instance, Ref. [86], or for the penetration depth, for instance, Ref. [87]). However, the fact that all these papers rely upon specific combinations of parameters, while the phenomena they seek to describe are rather universal, calls for caution. Besides, except in the pure unitary regime, scattering is accompanied by a T_c suppression and most papers do not find any correlation between thermodynamic probes and T_c among different samples. Another possibility is that required scattering is provided not by impurities, but by intrinsic defects that are thermodynamically or kinetically necessarily present in all samples (for example, dynamic domain walls introduced in Ref. [22]). More measurements at the lower temperature and on clean samples will probably clarify the matter. At the moment one cannot consider this problem solved.

Close to the thermodynamic measurements are tunneling type experiments. As of now, these have been nearly exclusively point-contact Andreev reflection probes. Here, again, the experimental reports are quite inconsistent, moreover, the situation is in some sense worse than in thermodynamic probes, since uncontrollable surface properties enter the picture. Interpretation generally includes fitting one curve with a large number of parameters, and the procedure is not always well defined. Generally speaking, three types of results have been reported: *d*-wave like, single full gap-like, and multi-gap. Interpretation is particularly difficult because within the $s^{\pm}$ picture formation of subgap Andreev bound states was predicted (*e.g.*, Refs. [88,89]) that can be easily mistaken for multiple gaps.

4.3. Phase-sensitive probes

In view of all that, experiments directly probing the gap symmetry are highly desirable. The paramagnetic Meissner effect, also known as *Wohlleben effect*, occurs in a polycrystalline sample when inter-grain weak links have random order parameter phase shifts, *0* or π. It has been routinely observed in cuprates and is considered a key signature of *d*-wave superconductivity. The effect does not exist in conventional, even anisotropic and multi-gap superconductors, even though sometimes it can be emulated by impurity effects in the junctions. For *d*-wave superconductors without pronounced crystallographic texture the Wohlleben effect is expected, and its absence can be taken as evidence against *d*-wave. Finally, in the $s^{\pm}$ scenario the phase is the same by symmetry for (100) and (010) grain boundaries, and there are good reasons to expect the same phase for (110) boundaries as well. There may or may not be a π phase shift for phase boundaries at some specific orientation, likely for a narrow range of angles [90], but probably not enough to produce a measurable Wohlleben effect. The absence of the effect in experiment [91] is a significant argument against *d*-wave, but hardly helps to distinguish *s* from $s^{\pm}$.

Similarly, the *c*-axis tunneling provides evidence against the *d*-wave, where the Josephson current strictly parallel to the crystallographic *c* direction vanishes by symmetry. Experimentally a sizable current was found [92].

Recalling the cuprates again, the ultimate argument in favor of the *d*-wave was provided by the corner Josephson junction experiments that probe directly the phase shift between two separate junctions; in cuprates, with their $d_{x^2-y^2}$ symmetry, these junction were to be along the (100) and (010) directions. Similarly, a potential d_{xy} state could be detected by the combination of (110) and $(\bar{1}10)$ directions. On the other hand, a conventional *s* state would not produce a phase shift for any combination of contacts. Again, the case of $s_{\pm}$ superconductivity is nontrivial. While symmetry does not mandate a π shift for any direction, it can be shown that, depending on the electronic structure parameters and properties of the interface, there may exist intermediate angles (between 0° and 45°) where a π shift is possible [90]. It also may be possible if the two junctions have different tunneling properties, so that one of them filters through only hole-pocket electrons, and the other only electron-pockets. It is not as bizarre as it may seem, and some possibilities were discussed in Ref. [90]. Probably the most promising design involves "sandwiches" of various geometries. The first proposal of that kind was by Tsoi et al. [89], who suggested an $s/s^{\pm}/s'$ trilayer, where *s* is a conventional quai-2D superconductor with a large Fermi surface that has no overlap with the hole FS of the $s^{\pm}$ layer (equivalently, a superconductor with small Fermi surfaces centered around the M points), and s' is a conventional superconductor with a small FS centered around Γ. This was followed by another proposal of a bilayer of hole-doped and electron-doped 122 materials [90]. In both cases the idea is that the current through the top of the sandwich will be dominated by the electron FS, and through the bottom by the hole one. Both proposals require momentum conservation in the interfacial plane, that is, basically, epitaxial or very high quality interface. The former proposal has an additional disadvantage of requiring *two* high-quality interfaces with very special conventional superconductors, particularly the one that should filter through the electron FS is rather difficult to find. As of now, no experiments have been reported pursuing any of the above suggestions, but with better single crystals and thin films it should become increasingly doable. It should be stressed, however, that in this case, unlike the cuprates, an absence of the π shifts in any of the proposed geometries does not disprove the $s^{\pm}$ scenario, since the effect here is quantitative rather than qualitative, but the presence of the sought effect would be a very strong argument in favor of it. On the other hand, standard 90° corner junction experiments similar to cuprates are also important, as they could prove unambiguously that the symmetry is not *d*-wave (even though they cannot distinguish between *s* and $s^{\pm}$). Preliminary result suggest an absence of the π-shifts in 90° junctions [104].

Further properties of interfaces between an $s^{\pm}$ superconductor and normal metal or conventional superconductor are now actively being studied theoretically, encouraging further experimental research. Probably we will see first results within the next year.

4.4. Coherence factor effects

Other signatures of the $s^{\pm}$ state are based on the fact, previously pointed out by many in connection with the cuprates, that the coherence factors are "reversed" for electronic transitions involv-

ing order parameters of the opposite sign. In the conventional BCS theory, as is well known, coherence factors of two kinds appear. The first kind, sometimes called "Type I" or "minus" coherence factor, is given by the expression $(1-\Delta_{\mathbf{k}}\Delta_{\mathbf{k}'}/E_{\mathbf{k}}E_{\mathbf{k}'})$, where $E_{\mathbf{k}}=\sqrt{\Delta_{\mathbf{k}}^2+\varepsilon_{\mathbf{k}}^2}$, and $\varepsilon_{\mathbf{k}}$ in the normal state excitation. The other kind, Type II or the "plus" coherence factor has the opposite sign in front of the fraction. If both order parameters entering this formula have the same sign, the Type I factor is destructive, in the sense that it goes to zero when $\varepsilon\to 0$, and cancels out the peak in the superconducting DOS. Type I factors appear, for instance, in the polarization operator, and as a result there are no coherence peaks in phonon renormalization (as measured by ultrasound attenuation, for instance) and in spin susceptibility (including the Knight shift). Type II factors appear, for instance, in the NMR relaxation rate, and they are constructive, resulting in the famous Hebel–Slichter peak below T_c.

Obviously, if $\Delta_{\mathbf{k}}$ and $\Delta_{\mathbf{k}'}$ have opposite signs, the meaning of the coherence factors is reversed; the Type I factors are now constructive and the Type II destructive. There are several straightforward ramifications of that. For instance, as it was pointed out already in the first paper proposing the $s^{\pm}$ scenario [5], the spin susceptibility at the SDW wave vector should show resonance enhancement just below T_c. For explicit calculations of this effect see for example Refs. [93,94]. There are indeed some reports of this effect, as measured by neutron scattering [95]. In principle, one can expect a similar effect in the phonon line-width, for the phonons with the same wave vector, just below T_c, but this is really hard to observe.

Less straightforward are cases of the quantities that involve averaging over the entire Brillouin zone, in which case the answer, essentially, depends on which processes play a more dominant role in the measured quantity, those involving intra-, or interband scattering. The answer usually depends on additional assumptions about the matrix elements involved, which can rarely be calculated easily from first principles. An example is electronic Raman scattering; a possibility of a resonant enhancement in some symmetries has been discussed recently [96].

5. Role of impurities

Impurity and defect scattering is believed to play an important role in pnictide superconductors. Proximity to a magnetic instability implies that ordinary defects may induce static magnetic moments on the neighboring Fe sites and thus trigger magnetic scattering. If, as is nearly universally believed, an order parameter with both signs is present, nonmagnetic impurities are also pair-breaking. Thus the anticipation is that in regular samples, and maybe in samples of much higher quality, impurity-induced pair-breaking will play a role.

Our intuition regarding the impurity effects in superconductors is largely based upon the Abrikosov–Gorkov theory of Born-scattering impurities in BCS superconductors. There was an observation at that time that folklore ascribes to Mark Azbel: Soviet theorists do what can be done as good as it should be done, and American ones do what shall be done as good as it could be done. For many years the approach to the impurity effects in superconductors was largely Soviet: most researchers refine the Abrikosov–Gorkov theory, applying it to anisotropic gaps and to unconventional superconductors, and relatively little has been done beyond the Born limit—despite multiple indications that most interesting superconductors, from cuprates to MgB_2 to pnictides are in the unitary limit or in an intermediate regime.

The physics of the nonmagnetic scattering in the two different limits is quite different. In the Born limit, averaging over all scattering events yields a spatially uniform superconducting state and tries to reduce the variation of the order parameter over the FS. Ultimately, for sufficiently strong scattering, the order parameter becomes a constant, corresponding to the DOS-weighted average over the FS. Note that unless this average is zero by symmetry (like in d-wave) the suppression of T_c, while linear at small concentrations, is never complete. As pointed out by Mishra et al. [97], this effect should manifest itself most clearly in an extended s-wave pairing with accidental nodes in the order parameter. Indeed, while in d-wave superconductors impurities broadens nodes into finite gapless spots, in an extended s case it is likely that the order parameter of one particular sign dominates a given FS pocket, in which case Born impurities will first make the parts of the FS with the "wrong" order parameter gapless, and then lead to a fully gapped superconductivity. Of course, this only holds for nonmagnetic impurities. Isotropic magnetic impurities will be just pair-breaking as they are in conventional superconductors, with the only interesting new physics being that magnetic impurities cease being pair-breakers if they scatter a pair such that the sign of the order parameter is flipping. The rule of thumb is that a scattering path for which magnetic scattering is pair-breaking (no change of sign of the order parameter), nonmagnetic scattering will not be pair-breaking, and *vice versa*.

The physics of the unitary limit is quite different. In that limit, the concentration of impurities is relatively low, but the scattering potential of an individual impurity is strong, $N(0)v_{imp}\gg 1$. In that case rather than suppressing superconductivity uniformly each impurity creates a bound state at the chemical potential, thus creating a zero energy peak in the density of states, without substantial suppression of the bulk superconductivity. Increasing the impurity concentration broadens the peak, while increasing its strength barely has any effect at all [98]. In an intermediate case between the Born limit and the unitary limit, the bound state is formed inside the gap at a finite energy and is the broader the closer it is to the gap (that is, closer to the Born limit).

The principal difference from the point of view of the experiment is that the unitary or intermediate scattering can create subgap density of states at arbitrary low energy at any temperature, without a drastic suppression of T_c. It was shown in Ref. [86] that any standard code for solving the Eliashberg equations in the Born limit can be easily modified, with minor changes, to treat the unitary limit, as well as any intermediate regime. Therefore we anticipate an imminent shift in the community from the "Soviet" approach to the "Western" approach, with more quantitative understanding of the effect beyond the Born approximation.

6. Conclusions

In this article we presented a brief overview of some proposals that have been made for the pairing state in the Fe-pnictide superconductors. In particular, we summarized arguments that support the view that the vicinity of superconductivity and magnetism in these systems is not accidental. The obvious appeal of this, and essentially any other electronic pairing mechanism is, of course, that the involved energy scales, and thus T_c, can in principle be larger if compared to pairing due to electron–phonon interaction. Electronic mechanisms also promise a new level of versatility in the design of new superconductors.

At this early stage in the research on the iron pnictide family, experiments have not conclusively determined the pairing symmetry, the detailed pairing state or the microscopic pairing mechanism. Still, in our view a plausible picture emerges where superconductivity is caused by magnetic fluctuations. Only two ingredients are vital to arrive at a rather robust conclusion for the pairing state. First, pnictides need to have Fermi surface sheets of two kinds, one near the center of the Brillouin zone, and the other near the corner. Second, the typical momentum for the mag-

netic fluctuations should be close to the ordering vectors $\mathbf{Q} = (\pi, \pi)$ of the parent compounds. Then, magnetic interactions lead quite naturally to an efficient interband coupling that yields an $s^{\pm}$ pairing state. This result is general in the sense that it is obtained regardless of whether one develops a theory based on localized quantum magnetism or itinerant paramagnons. There is evidence that the two needed ingredients are present in the pnictides. Fermi surface sheets at the appropriate locations have been predicted in non-magnetic LDA calculations and seen in ARPES experiments. The magnetic ordering vector has been determined via neutron scattering, even though we have to stress that a clear identification of magnetic fluctuations for superconducting systems without long-range magnetic order is still lacking.

The resulting $s^{\pm}$ pairing state has a number of interesting properties. As far as the a group theoretic classification is concerned, its symmetry is the same as that for a conventional s-wave pairing, where the gap-function has same sign on all sheets of the Fermi surface. However, there are significant differences between the two states. The sign change in the gap affects the coherence factors, leading to the resonance peak in the dynamic spin susceptibility and the absence of a Hebel–Slichter peak in NMR. Nonmagnetic impurities affect the $s^{\pm}$-state just like magnetic impurities do in an ordinary s-wave state, i.e. here a behavior more akin to d-wave superconductors. Another implication of the sign change in the $s^{\pm}$-state leads to rather efficient Coulomb avoidance.

The presence of nodes in the superconducting gap in still an open issue. In d-wave or p-wave pairing states, nodal lines or points are fixed by symmetry. This is different for the $s^{\pm}$-state. In its most elementary version, the sign change of the gap corresponds to a node located between two Fermi surface sheets. This is the case for the $\Delta(\mathbf{k})$ given in Eq. (3). Energetic arguments favor such a gapless state as long as the momentum transfer $\mathbf{Q}$ couples efficiently to large parts of distinct Fermi surface sheets and Coulomb avoidance is efficient. However, as there is no symmetry constraint for the location of the nodes, it is in principle possible that there are nodes on some Fermi surface sheets.

Next to the nature of the pairing state, the microscopic understanding of the magnetism of the Fe-pnictides is one of the most interesting aspects of these materials. Are these systems made up of localized spins that interact via short ranged, nearest neighbor exchange interactions or, are they better described in terms of itinerant magnetism? While we emphasized that many aspects of the pairing state emerge regardless of which of these points of view is correct, this is really only true for the most elementary aspects of the theory. As our understanding of these materials deepens, dynamical aspects of the pairing state will become more and more important, and the details of the magnetic degrees of freedom will matter. In our view, the most sensible description starts from itinerant electrons, however with significant electron–electron interaction. In detail, we find numerous arguments that emphasize the role of magneto-elastic couplings and that favor a sizable Hund coupling, i.e. the multi orbital character and the corresponding local multi-orbital interactions are important to understand the magnetism and superconductivity alike. Regardless of whether this specific point of view is correct or not, it is already evident that the ferropnictides make up a whole new class of materials that stubbornly refuse to behave according to one of the simple minded categories of condensed matter theory.

Acknowledgements

This research was supported by the Ames Laboratory, operated for the US Department of Energy by Iowa State University under Contract No. DE-AC02-07CH11358 (J.S.), and by the Office of Naval Research (I.I.M.). The authors wish to thank all their friends and collaborators, without whom this works could not be accomplished, and their numerous colleagues who read the manuscript and sent us many useful and insightful comments.

References

[1] X. Marchan, W. Jeitschko, J. Solid State Chem. 24 (1978) 351.
[2] Y. Kamihara, T. Watanabe, M. Hirano, H. Hosono, J. Am. Chem. Soc. 130 (2008) 3296.
[3] M. Rotter, M. Tegel, D. Johrendt, Phys. Rev. Lett. 101 (2008) 107006.
[4] All original calculations used in this article were performed using the standard full-potential LAPW package WIEN2k. The details can be found in Refs. [5,99]. Unless stated otherwise, the experimental crystal structure is used.
[5] I.I. Mazin, D.J. Singh, M.D. Johannes, M.H. Du, Phys. Rev. Lett. 101 (2008) 057003.
[6] C. Liu, T. Kondo, M.E. Tillman, R. Gordon, G.D. Samolyuk, Y. Lee, C. Martin, J.L. McChesney, S. Bud'ko, M.A. Tanatar, E. Rotenberg, P.C. Canfield, R. Prozorov, B.N. Harmon, A. Kaminski, arxiv:0806.2147.
[7] T. Kondo, A.F. Santander-Syro, O. Copie, Chang Liu, M.E. Tillman, E.D. Mun, J. Schmalian, S.L. Bud'ko, M.A. Tanatar, P.C. Canfield, A. Kaminski, Phys. Rev. Lett. 101 (2008) 147003.
[8] H. Ding, P. Richard, K. Nakayama, K. Sugawara, T. Arakane, Y. Sekiba, A. Takayama, S. Souma, T. Sato, T. Takahashi, Z. Wang, X. Dai, Z. Fang, G.F. Chen, J.L. Luo, N.L. Wang, Europhys. Lett. 83 (2008) 47001.
[9] L. Zhao, H. Liu, W. Zhang, J. Meng, X. Jia, G. Liu, X. Dong, G.F. Chen, J.L. Luo, N.L. Wang, G. Wang, Y. Zhou, Y. Zhu, X. Wang, Z. Zhao, Z. Xu, C. Chen, X.J. Zhou, Chin. Phys. Lett. 25 (2008) 4402.
[10] L. Wray, D. Qian, D. Hsieh, Y. Xia, L. Li, J.G. Checkelsky, A. Pasupathy, K.K. Gomes, C.V. Parker, A.V. Fedorov, G.F. Chen, J.L. Luo, A. Yazdani, N.P. Ong, N.L. Wang, M.Z. Hasan, Phys. Rev. B 78 (2008) 184508.
[11] K. Nakayama, T. Sato, P. Richard, Y.-M. Xu, Y. Sekiba, S. Souma,G.F. Chen, J.L. Luo, N.L. Wang, H. Ding, T. Takahashi, arxiv:0812.0663.
[12] A.P. Mackenzie, S.R. Julian, A.J. Diver, G.G. Lonzarich, N.E. Hussey, Y. Maeno, S. Nishizaki, T. Fujita, Physica C 263 (1996) 510.
[13] G. Mu, H. Luo, Z. Wang, Z. Ren, L. Shan, C. Ren, H.-H. Wen, arxiv:0812.1188.
[14] The experiment was performed at the nominal doping of 0.1e; in the calculations[4], the DOS drops sharply from 2.1 st/eV f.u. to 1.5 st./eV f.u. at $x \approx 0.15$. The former value corresponds to renormalization between 1 and 1.2, and the latter to 1.5–2.
[15] J.K. Dong, L. Ding, H. Wang, X.F. Wang, T. Wu, X.H. Chen, S.Y. Li, arxiv:0806.3573.
[16] A.I. Coldea, J.D. Fletcher, A. Carrington, J.G. Analytis, A.F. Bangura, J.-H. Chu, A.S. Erickson, I.R. Fisher, N.E. Hussey, R.D. McDonald, Phys. Rev. Lett. 101 (2008) 216402.
[17] D.H. Lu, M. Yi, S.-K. Mo, A.S. Erickson, J. Analytis, J.-H. Chu, D.J. Singh, Z. Hussain, T.H. Geballe, I.R. Fisher, Z.-X. Shen, Nature 455 (2008) 81.
[18] S.E. Sebastian, J. Gillett, N. Harrison, P.H.C. Lau, C.H. Mielke, G.G. Lonzarich, J. Phys.: Condens. Matter 20 (2008) 422203. and unpublished.
[19] J.G. Analytis, I.R. Fisher, et al., unpublished.
[20] K. Terashima, Y. Sekiba, J.H. Bowen, K. Nakayama, T. Kawahara, T. Sato, P. Richard, Y.-M. Xu, L.J. Li, G.H. Cao, Z.-A. Xu, H. Ding, T. Takahashi, arxiv:0812.3704.
[21] K. Matan1, R. Morinaga, K. Iida, T.J. Sato, Phys. Rev. B 79 (2009) 054526.
[22] I.I. Mazin, M.D. Johannes, Nature Phys. (2009).
[23] M.A. McGuire, A.D. Christianson, A.S. Sefat, B.C. Sales, M.D. Lumsden, R. Jin, E.A. Payzant, D. Mandrus, Y. Luan, V. Keppens, V. Varadarajan, J.W. Brill, R.P. Hermann, M.T. Sougrati, F. Grandjean, G.J. Long, Phys. Rev. B 78 (2008) 094517.
[24] Y. Chen, J.W. Lynn, J. Li, G. Li, G.F. Chen, J.L. Luo, N.L. Wang, P. Dai, C. dela Cruz, H.A. Mook, Phys. Rev. B 78 (2008) 064515.
[25] J. Zhao, Q. Huang, Cl. de la Cruz, S. Li, J.W. Lynn, Y. Chen, M.A. Green, G.F. Chen, G. Li, Z. Li, J.L. Luo, N.L. Wang, P. Dai, Nature Mater. 7 (2008) 953.
[26] Q. Huang, Y. Qiu, W. Bao, J.W. Lynn, M.A. Green, Y. Chen, T. Wu, G. Wu, X.H. Chen, Phys. Rev. Lett. 101 (2008) 257003.
[27] Y. Qiu, W. Bao, Q. Huang, T. Yildirim, J. Simmons, J.W. Lynn, Y.C. Gasparovic, J. Li, M. Green, T. Wu, G. Wu, X.H. Chen, Phys. Rev. Lett. 101 (2008) 257002.
[28] J. Dong, H.J. Zhang, G. Xu, Z. Li, G. Li, W.Z. Hu, D. Wu, G.F. Chen, X. Dai, J.L. Luo, Z. Fang, N.L. Wang, Europhys. Lett. 83 (2008) 27006.
[29] W.Z. Hu, J. Dong, G. Li, Z. Li, P. Zheng, G.F. Chen, J.L. Luo, N.L. Wang, Phys. Rev. Lett. 101 (2008) 257005.
[30] D. Hsieh, Y. Xia, L. Wray, D. Qian, K. Gomes, A. Yazdani, G.F. Chen, J.L. Luo, N.L. Wang, M.Z. Hasan, arxiv:0812.2289.
[31] X.F. Wang, T. Wu, G. Wu, H. Chen, Y.L. Xie, J.J. Ying, Y.J. Yan, R.H. Liu, X.H. Chen, arxiv:0806.2452.
[32] Not only the energetics of collinear LDA calculations cannot be mapped upon a $J_1 + J_2$ model [99] (one requires forced FM calculations, but it was also directly demonstrated by noncollinear LDA calculations by Stuttgart group [101]).
[33] W. Bao, Y. Qiu, Q. Huang, M.A. Green, P. Zajdel, M.R. Fitzsimmons, M. Zhernenkov, M. Fang, B. Qian, E.K. Vehstedt, J. Yang, H.M. Pham, L. Spinu, Z.Q. Mao, arxiv:0809.2058.
[34] DFT calculations [4] yield the following magnetic stabilization energies for FeTe: 332 (227) meV/Fe with (without) spin-orbit coupling in the experimental P21/m double-stripe structure, and 281 (205) meV/Fe with in the single-stripe Pccm structure (with full optimization of atomic positions in

each structure). Thus, the experimental structure appears to be below the competing structure by 22 (or 49, with spin-orbit) meV/Fe. Exactly the same calculation for LaFeAsO [99] render the double-stripe structure well above the single-stripe one. The difference can be traced down to the fact that for LaFeAsO only the single stripe structure opens a pseudogap in DOS at the Fermi level, while for FeTe both AFM structures open comparable pseudogaps. Further details will be published elsewhere [100].
[35] T. Kroll, S. Bonhommeau, T. Kachel, H.A. Dürr, J. Werner, G. Behr, A. Koitzsch, R. Hübel, S. Leger, R. Schönfelder, A. Ariffin, R. Manzke, F.M.F. de Groot, J. Fink, H. Eschrig, B. Büchner, M. Knupfer, Phys. Rev. B 78 (2008) 220502(R).
[36] K. Haule, G. Kotliar, New J. Phys. 11 (2009) 025021.
[37] F. Wang, H. Zhai, D. Lee, Europhys. Lett. 85 (2009) 37005.
[38] A.V. Chubukov, D. Efremov, I. Eremin, Phys. Rev. B 78 (2008) 134512.
[39] V. Stanev, J. Kang, Z. Tesanovic, Phys. Rev. B 78 (2008) 184509.
[40] K. Kuroki, S. Onari, R. Arita, H. Usui, Y. Tanaka, H. Kontani, H. Aoki, Phys. Rev. Lett. 101 (2008) 087004.
[41] S. Graser, G.R. Boyd, C. Cao, H.-P. Cheng, P.J. Hirschfeld, D.J. Scalapino, Phys. Rev. B 77 (2008) 180514(R).
[42] S. Graser, T.A. Maier, P.J. Hirschfeld, D.J. Scalapino, New J. Phys. 11 (2009) 025016.
[43] X.-L. Qi, S. Raghu, C.-X. Liu, D.J. Scalapino, S.-C. Zhang, arxiv:0804.4332.
[44] Z.-J. Yao, J.-X. Li, Z.D. Wang, New J. Phys. 11 (2009) 025009.
[45] R. Sknepnek, G. Samolyuk, Y. Lee, J. Schmalian, Phys. Rev. B 79 (2009) 054511.
[46] N.E. Bickers, D.J. Scalapino, S.R. White, Phys. Rev. Lett. 62 (1989) 961.
[47] Ar. Abanov, A.V. Chubukov, J. Schmalian, Adv. Phys. 52 (2003) 119.
[48] Q. Si, E. Abrahams, Phys. Rev. Lett. 101 (2008) 076401.
[49] Experimentally observed Drude weight is sizeable above the Neel temperature ($\omega_p > 1.5$ eV). Some researchers report substantial reduction of the Drude weight in the antiferromagnetic state, consistent with Fermi surface gapping, (W.Z. Hu, Q.M. Zhang, N.L. Wang, this issue, doi:10.1016/j.physc.2009.03.047), while other do not see such large reduction (F. Pfuner, J.G. Analytis, J.-H. Chu, I.R. Fisher, L. Degiorgi, European Phys. J. B67, 513, 2009).
[50] C. Fang, H. Yao, W.-F. Tsai, J. Hu, S.A. Kivelson, Phys. Rev. B 77 (2008) 224509.
[51] C. Xu, M. Mueller, S. Sachdev, Phys. Rev. B 78 (2008) 020501(R).
[52] T. Yildirim, Phys. Rev. Lett. 101 (2008) 057010.
[53] D.J. Singh, M.H. Dur, Phys. Rev. Lett. 100 (2008) 237003.
[54] See, for instance, I.I. Mazin, Phys. Rev. B 75 (2007) 094407.
[55] S. Sachdev, Physica A 313 (2002) 252.
[56] K. Seo, B.A. Bernevig, J. Hu, Phys. Rev. Lett. 101 (2008) 206404.
[57] L. Boeri, O.V. Dolgov, A.A. Golubov, Phys. Rev. Lett. 101 (2008) 026403.
[58] F. Yndurain, J.M. Soler, arxiv:0810.2474.
[59] M. Rotter, M. Tegel, D. Johrendt, I. Schellenberg, W. Hermes, R. Poettgen, Phys. Rev. B 78 (2008) 020503(R).
[60] N. Ni, S. Nandi, A. Kreyssig, A.I. Goldman, E.D. Mun, S.L. Bud'ko, P.C. Canfield, Phys. Rev. B 78 (2008) 014523.
[61] A. Jesche, N. Caroca-Canales, H. Rosner, H. Borrmann, A. Ormeci, D. Kasinathan, H.H. Klauss, H. Luetkens, R. Khasanov, A. Amato, A. Hoser, K. Kaneko, C. Krellner, C. Geibel, Phys. Rev. B 78 (2008) 180504(R).
[62] G.D. Samolyuk, V.P. Antropov, Phys. Rev. B 79 (2009) 052505.
[63] P. Chandra, P. Coleman, A.I. Larkin, Phys. Rev. Lett. 64 (1990) 88.
[64] In reality there is no such degeneracy even on the mean-field level, reflecting the fact that, as discussed above, actual DFT calculations cannot be mapped upon a $J_1 + J_2$ model. As shown by Yaresko et al. [101], mutually orthogonal sublattices calculate to a have much larger energy than parallel.
[65] R. Fernandes, J. Schmalian, submitted for publication.
[66] K. Kaneko, A. Hoser, N. Caroca-Canales, A. Jesche, C. Krellner, O. Stockert, C. Geibel, Phys. Rev. B 78 (2008) 212502.
[67] C. Geibel, private communication.
[68] V. Barzykin, L.P. Gor'kov, JETP. Lett. 88 (2008) 131.
[69] W.A. Little, Phys. Rev. 134A (1964) 1416;
W.A. Little, Phys. Rev. 156 (1967) 396.
[70] V.L. Ginzburg, D.A. Kirzhnits, Soviet Phys.—JETP 19 (1964) 269.
[71] M. Berciu, I. Elfimov, G.A. Sawatzky, arxiv:0811.0214.
[72] D.F. Agterberg, V. Barzykin, L.P. Gor'kov, Phys. Rev. B 60 (1999) 14868.
[73] F. Ning, K. Ahilan, T. Imai, A.S. Sefat, R. Jin, M.A. McGuire, B.C. Sales, D. Mandrus, J. Phys. Soc. Jpn. 77 (2008) 103705.
[74] N. Terasaki, H. Mukuda, M. Yashima, Y. Kitaoka, K. Miyazawa, P. Shirage, H. Kito, H. Eisaki, A. Iyo, arxiv:0809.5155.
[75] Y. Nakai, K. Ishida, Y. Kamihara, M. Hirano, H. Hosono, J. Phys. Soc. Jpn. 77 (2008) 073701.
[76] S. Kawasaki, K. Shimada, G.F. Chen, J.L. Luo, N.L. Wang, G.-q. Zheng, Phys. Rev. B 78 (2008) 220506.
[77] Y. Kobayashi, A. Kawabata, S.C. Lee, T. Moyoshi, M. Sato, arxiv:0901.2830.
[78] H. Fukazawa, T. Yamazaki, K. Kondo, Y. Kohori, N. Takeshita, P.M. Shirage, K. Kihou, K. Miyazawa, H. Kito, H. Eisaki, A. Iyo, arxiv:0901.0177.
[79] Y. Nakai, K. Ishida, Y. Kamihara, M. Hirano, H. Hosono, Phys. Rev. Lett. 101 (2008) 077006.
[80] K. Hashimoto, T. Shibauchi, T. Kato, K. Ikada, R. Okazaki, H. Shishido,M. Ishikado, H. Kito, A. Iyo, H. Eisaki, S. Shamoto, Y. Matsuda, arxiv:0806.3149.
[81] L. Malone, J.D. Fletcher, A. Serafin, A. Carrington, N.D. Zhigadlo, Z. Bukowski, S. Katrych, J. Karpinski, Phys. Rev. Lett. 102 (2009) 017002.
[82] C. Martin, R.T. Gordon, M.A. Tanatar, M.D. Vannette, M.E. Tillman, E.D. Mun, P.C. Canfield, V.G. Kogan, G.D. Samolyuk, J. Schmalian, R. Prozorov, Phys. Rev. B 79 (2009) 100506(R), and unpublished.
[83] R. Prozorov, M.A. Tanatar, R.T. Gordon, C. Martin, H. Kim, V.G. Kogan, N. Ni, M.E. Tillman, S.L. Bud'ko, P.C. Canfield, arxiv:0901.3698.
[84] R.T. Gordon, C. Martin, H. Kim, N. Ni, M.A. Tanatar, J. Schmalian, I.I. Mazin, S.L. Bud'ko, P.C. Canfield, R. Prozorov, arxiv:0812.3683.
[85] J.D. Fletcher, A. Serafin, L. Malone, J. Analytis, J.-H. Chu, A.S. Erickson, I.R. Fisher, A. Carrington, arxiv:0812.3858.
[86] D. Parker, O.V. Dolgov, M.M. Korshunov, A.A. Golubov, I.I. Mazin, Phys. Rev. B 78 (2008) 134524.
[87] A.B. Vorontsov, M.G. Vavilov, A.V. Chubukov, arxiv:0901.0719.
[88] A.A. Golubov, A. Brinkman, O.V. Dolgov, I.I. Mazin, Y. Tanaka, arxiv:0812.5057.
[89] W.-F. Tsai, D.-X. Yao, B.A. Bernevig, J.P. Hu, arxiv:0812.0661.
[90] D. Parker, I.I. Mazin, arxiv:0812.4416.
[91] C.W. Hicks, T.M. Lippman, M.E. Huber, Z.A. Ren, Z.X. Zhao, K.A. Moler, J. Phys. Soc. Japan 78 (2009) 013708.
[92] X. Zhang, Y.S. Oh, Y. Liu, L. Yan, K.H. Kim, R.L. Greene, I. Takeuchi, arxiv:0812.3605.
[93] T. Maier, D.J. Scalapino, Phys. Rev. B 78 (2008) 20514(R).
[94] M.M. Korshunov, I. Eremin, Europhys. Lett. 83 (2008) 67003.
[95] A.D. Christianson, E.A. Goremychkin, R. Osborn, S. Rosenkranz, M.D. Lumsden, C.D. Malliakas, S. Todorov, H. Claus, D.Y. Chung, M.G. Kanatzidis, R.I. Bewley, T. Guidi, arxiv:0807.3932; M.D. Lumsden, A.D. Christianson, D. Parshall, M.B. Stone, S.E. Nagler, H.A. Mook, K. Lokshin, T. Egami, D.L. Abernathy, E.A. Goremychkin, R. Osborn, M.A. McGuire, A.S. Sefat, R. Jin, B.C. Sales, D. Mandrus, Nature 456 (2008) 930.
[96] A.V. Chubukov, I. Eremin, M.M. Korshunov, arxiv:0901.2102.
[97] V. Mishra, G. Boyd, S. Graser, T. Maier, P.J. Hirschfeld, D.J. Scalapino, arxiv:0901.2653.
[98] G. Preosti, P. Muzikar, Phys. Rev. B 54 (1996) 3489.
[99] I.I. Mazin, M.D. Johannes, L. Boeri, K. Koepernik, D.J. Singh, Phys. Rev. B 78 (2008) 085104.
[100] M.D. Johannes, I.I. Mazin, arXiv:0904.3857.
[101] A.N. Yaresko, G.-Q. Liu, V.N. Antonov, O.K. Andersen, arxiv:0810.4469.
[102] I.I. Mazin, Physica C 468 (2008) 105.
[103] O.V. Dolgov, I.I. Mazin, D. Parker, A.A. Golubov, Phys. Rev. B 79 (2009) 060502(R) (Rapid Communication).
[104] Y.-R. Zhou, Y.-R. Li, J.-W. Zuo, R.-Y. Liu, S.-K. Su, G.F. Chen, J.L. Lu, N.L. Wang, Y.-P. Wang, arXiv:0812.3295 (2008).